Risks From Spacecraft Breakup Events in Near Rectilinear Halo Orbits

Nathan R. Boone, **Robert A. Bettinger**, **Bryan D. Little**
Air Force Research Laboratory

ABSTRACT

Spacecraft breakup events were simulated in the vicinity of the Lunar Gateway's Near Rectilinear Halo Orbit to evaluate the risk of debris collision with the station. The Monte Carlo simulations model the breakup of an object shortly after deployment from the Gateway, and using the propagated trajectories of over a million particles across 5,000 random breakup events, the likelihood of collision with the Gateway is statistically evaluated. Approaches within 10 km were observed for only 2.4% of the breakup events, suggesting a low risk of collision, but approaches at larger distances that might still generate a debris avoidance maneuver were relatively likely. Changes in velocity at deployment of above 4 m/s appeared to lower the risk of collision. The risk was highest at about 1.57 days after the breakup but dropped rapidly as the vast majority of objects departed the Near Rectilinear Halo Orbit within weeks. After one year, about 20% of the fragments had impacted the Moon, 61% had escaped the Earth-Moon system, and 19% remained elsewhere in cislunar space. Few objects would intersect useful near-Earth orbits and there were very few Earth impacts. The results of this study provide quantifiable insight into the risk of debris collision with the Gateway that can be used to develop operational plans to mitigate this risk.

1. INTRODUCTION

Interest in cislunar space has swelled in recent years, and nations such as the United States, Russia, and China have developed plans for ambitious cislunar space missions. These include plans for crewed cislunar space stations, lunar landings, and lunar bases. Additional cislunar spacecraft are likely to be required to support the growing number of missions, especially to extend Space Situational Awareness (SSA), communication, and navigation capabilities capabilities beyond Geostationary Earth Orbit (GEO) [1]. The United States has been vocal about the need to expand space operations into cislunar space, and the White House National Cislunar Science and Technology Strategy, released in November 2022, calls for extending SSA capabilities into cislunar space, expanding international cooperation, supporting cislunar research and development, and developing cislunar communications and navigation infrastructure [2].

As more spacecraft have begun to operate in cislunar space, some have raised concerns over potential problems with artificial debris in useful cislunar orbits. The White House Cislunar Strategy specifically mentions the need to avoid debris in cislunar space, stating that the United States government will "aim to understand the long-term effects of growing human activities on the Cislunar environment, and to preserve a safe and sustainable environment in Cislunar space - such as limiting space debris in Lunar orbit." The Cislunar Strategy calls for developing debris mitigation strategies, standards for End of Life (EOL) disposal, a cislunar object catalog, and cislunar SSA capabilities to track debris [2]. Pollock and Vedda [3] also expressed concerns that certain useful cislunar orbits, such as Near Rectilinear Halo Orbits (NRHOs), may someday become congested, and called for the early establishment of cislunar debris guidelines to avoid later costly remediation.

NRHOs have potentially significant utility for future lunar exploration. The crewed Lunar Gateway space station will operate in a NRHO, with construction planned to start in the late 2020s [1]. The utility of NRHOs for future lunar exploration, and especially their planned use to support crewed spacecraft, makes it important to study the propagation

of debris in these orbits. Several existing studies have investigated debris-generating breakup events in cislunar orbits [4, 5, 6, 7, 8], finding slight risks to other cislunar spacecraft and to orbital environments closer to Earth such as Low Earth Orbit (LEO) and GEO. Only Guardabasso et. al [8] considered debris in NRHOs, but this study did not utilize Monte Carlo breakup simulation to quantify the risk to the Gateway. Monte Carlo simulations are useful for analysis of space debris because they allow a characterization of the risk despite many uncertain variables, such as the breakup time, the breakup location, and the breakup properties [9, 10].

This paper describes Monte Carlo simulations of breakup events near the Gateway's NRHO and discusses the resulting risks from the debris to the Gateway. The simulations focus on a deployment scenario in which an object, such as a resupply module or satellite, suffers a breakup event following deployment from the station. The simulation results are generally applicable to any breakup event in the vicinity of the Gateway's NRHO, and include an analysis of the debris trajectories, the collision risks to the Gateway, and the final states of debris after the simulation completes. These results enable an analysis of the consequences of breakup events in the vicinity of the Gateway's NRHO, allowing the development of guidelines for safe space operations in this region.

2. METHODOLOGY

This section begins with a discussion of the cislunar dynamics relevant to the present study. The next subsection describes the Gateway reference trajectory, which was obtained from a published NASA ephemeris file. Next, the spacecraft breakup model is described. The final three subsections outline the high-fidelity orbit propagation, the simulation design, and the method for analyzing the collision risk, respectively.

2.1 Cislunar Dynamics

Cislunar dynamics are often approximated using the Earth-Moon Circular Restricted Three-Body Problem (CR3BP), which assumes that the mass of the spacecraft is negligible with respect to the Earth and the Moon, that the Earth and Moon move in coplanar circular orbits about their center of mass (or barycenter), and that the Earth and Moon move with constant angular velocities [11]. Although the CR3BP was not used for any orbit propagation in this study, the CR3BP still provides useful insight into cislunar dynamics, and trajectories that are stable according to the Earth-Moon CR3BP are often used in cislunar mission design. The CR3BP includes five stable *Lagrange points* at which gravitational forces balance, referred to as L_1, L_2, L_3, L_4, and L_5. The location of these Lagrange points is shown in the Earth-Moon barycentric rotating reference frame in Fig. 1. The units in this plot are non-dimensionalized such that one Distance Unit (DU) equals the assumed distance between the Earth and the Moon, 384,400 km. The L_1 and L_2 Lagrange points are especially useful because they are near the Moon and spacecraft can efficiently transfer from them to both the Earth and Moon [12].

Orbits about the Lagrange points are often called *halo orbits*. NRHOs are a particularly useful class of L_1 and L_2 halo orbits. These orbits are stable, are easily accessible from Earth, allow access to both the lunar surface and interplanetary destinations, and can provide communications coverage to one of the lunar poles for most of the orbit. An example NRHO is plotted in the Earth-Moon rotating frame centered at the Moon in Fig. 2. An L_2 South NRHO that completes an average of nine revolutions for every two lunar months was chosen as the operational orbit for the Lunar Gateway. This orbit has desirable characteristics such as good visibility of the lunar far side, favorable stability, a lower fuel cost for returns to Earth, and the ability to provide communication coverage to regions of interest at the lunar south pole. The Gateway orbit has also been carefully designed to minimize eclipses by the Earth [13].

The CR3BP includes a constant of the motion known as Jacobi's Constant, which provides insight into accessible and inaccessible regions of cislunar space. This constant is expressed as:

$$C = 2U - v^2 \tag{1}$$

where v is the object speed and the pseudopotential U is given by:

$$U = \frac{1-\mu}{\rho_E} + \frac{\mu}{\rho_M} + \frac{1}{2}\left(x^2 + y^2\right) \tag{2}$$

where ρ_E is the distance from the object to the Earth, ρ_M is the distance from the object to the Moon, x and y are the coordinates in the Earth-Moon barycentric rotating reference frame, and μ is a constant equal to 0.01215. All quantities are in non-dimensional units such that one DU is 384,400 km and one Time Unit (TU) is 4.3425 days. In

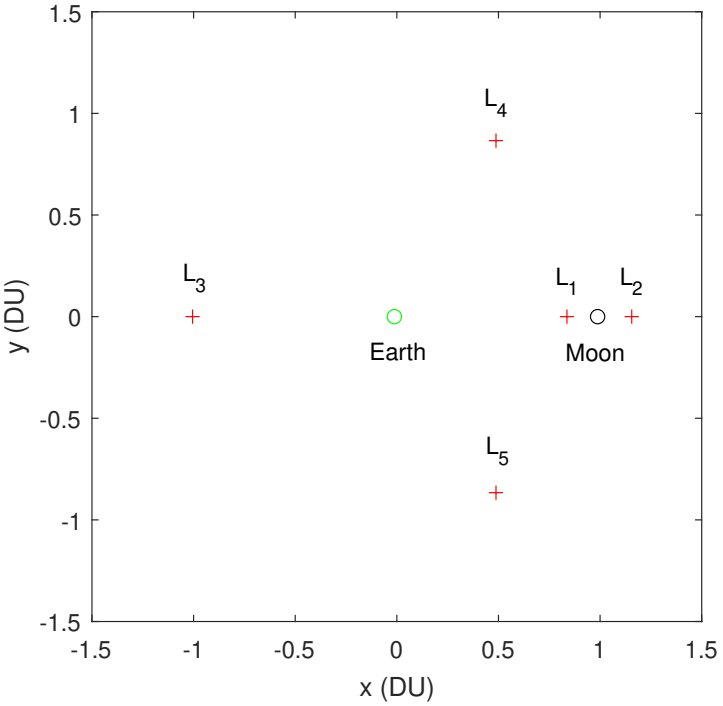

Fig. 1: Equilibrium Points in the Earth-Moon CR3BP

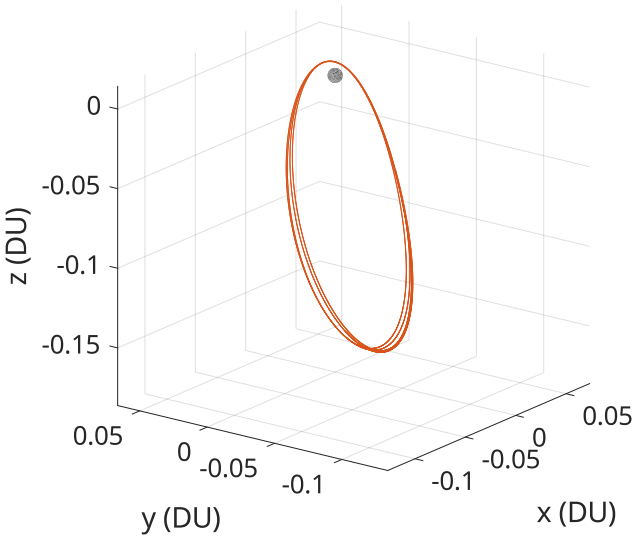

Fig. 2: Example NRHO

the CR3BP, the Jacobi Constant cannot be changed unless energy is added, such as through an engine burn. Locations in cislunar space where $v = 0$ for a given Jacobi Constant form boundaries known as Zero-Velocity Curves (ZVC) that cannot be crossed without the addition of energy. Although Jacobi's Constant is no longer constant in ephemeris-based trajectory models where the assumptions of the CR3BP are violated (as used in this study), the ZVC are still useful for describing the motion of cislunar debris objects.

2.2 Gateway Reference Trajectory

Breakup events were simulated in orbits near the Gateway's operational NRHO. The Gateway's operational orbit was obtained from the NASA's reference trajectory, discussed in Ref. [13]. The Gateway reference trajectory is provided as an ephemeris file that spans 15 years, from 2 January 2020 to 11 February 2035. The trajectory is continuous in position, but velocity adjustments occur to maintain the orbit. NASA's General Mission Analysis Tool (GMAT) was used to read the ephemeris file and obtain the Gateway's state at desired dates and times from the reference trajectory.

2.3 Breakup Model

The NASA Standard Breakup Model [14] was used to determine the properties of spacecraft breakup events. The NASA Standard Breakup Model is a statistical model that randomly generates fragment ejection velocities, masses, and sizes. An implementation of the breakup model identical to that used in Ref. [15] was used for this study, and the implementation is reviewed here.

The number of particles released from a spacecraft breakup event is governed by the power law equation:

$$N(L_c) = 6L_c^{-\beta} \tag{3}$$

where L_c is the minimum particle size considered in meters and β is a constant equal to 1.6. To place a practical limit the number of objects that must be propagated with each run of the simulation, only fragments with a characteristic length larger than 10 cm ($L_c > 0.1$) were considered in this study. Particles larger than 10 cm would be the most threatening to other spacecraft, and 10 cm is also the trackable limit of objects in the LEO environment [14], allowing comparisons with the trackable LEO debris environment. Equation (3) indicates that there will be approximately 238 particles of size 10 cm or larger.

The sizes of debris objects were generated using the following power law equation from Frey [16]:

$$\lambda = -\frac{1}{\beta}\log_{10}\left[10^{-\beta\lambda_0} - P_\lambda(10^{-\beta\lambda_0} - 10^{-\beta\lambda_1})\right] \tag{4}$$

where P_λ is a random variable uniformly distributed between 0 and 1. λ, λ_0, and λ_1 are given by:

$$\lambda = \log_{10}(L_c) \tag{5}$$

$$\lambda_0 = \log_{10}(L_{c_0}) \tag{6}$$

$$\lambda_1 = \log_{10}(L_{c_1}) \tag{7}$$

where L_{c_0} is the lower fragment characteristic length limit in meters (0.1) and L_{c_1} is the upper limit in meters. Krisko [17] indicated that the power law may break down for fragment sizes above 1 m, so 1 m was used as the upper characteristic length limit.

After determining particle characteristic lengths, the distribution functions provided by Johnson et al. [14] were used to calculate the fragment area-to-mass ratios. Another distribution function provided by Johnson et al. [14] was used to calculate the ejection speeds from the area-to-mass ratios. A direction can be assigned to the speed by assuming an omnidirectional explosion and picking a random point on a sphere [18]:

$$\Delta V_x = \Delta V\sqrt{1-u^2}\cos\theta \tag{8}$$

$$\Delta V_y = \Delta V\sqrt{1-u^2}\sin\theta \tag{9}$$

$$\Delta V_z = \Delta V u \tag{10}$$

where u is a random number uniformly sampled between -1 and 1, and θ is a random angle uniformly sampled between 0 and 2π.

Mass conservation was also enforced with an assumed pre-explosion mass of 800 kg. The NASA Standard Breakup Model does not guarantee mass conservation by default, typically generating too little mass relative to the original pre-explosion mass. Krisko [17] recommended enforcing mass conservation by generating two to eight additional fragments larger than 1 m. These objects would represent larger components not totally destroyed in the explosion such as pressurant tanks, nozzle bells, etc. Up to eight additional fragments in the characteristic length range $L_{c_0} = 1$ and $L_{c_1} = 5$, in meters, were randomly generated until the total fragment mass summed to 800 kg to within a tolerance of 5%. The assumed pre-explosion mass only affects the properties of these final two to eight particles.

This implementation of the NASA Standard Breakup Model generates between 239 and 246 particles for each breakup event, and the average ejection velocity is typically near 70 m/s. The fragment ejection velocities were used to determine the initial states of all objects, and the cross-sectional areas and masses of the particles were used for the solar radiation pressure (SRP) calculation in the orbit propagator. The fragments were assumed to have a coefficient of reflectivity of c_R = 1.2 based on another study that used this value to model the influence of SRP on debris fragments [19].

2.4 Orbit Propagation

Orbit propagation was required for determining the trajectories of the spacecraft that suffers the breakup event and of the resulting debris, and all orbit propagation in this study was accomplished using NASA GMAT. GMAT is an open-source space mission analysis tool developed by NASA that achieved its first flight-qualified release in 2013 [20]. GMAT was well-suited for this study due to its high-fidelity orbit propagation capabilities and its command-line interface. This enabled accurate and efficient propagation of hundreds of thousands of debris objects.

Most prior studies that used ephemeris-based cislunar trajectory models considered the point-mass gravity of the Earth and Sun, a non-spherical lunar gravity model with degree and order 8, and the force due to SRP [21, 22, 23, 24]. Development of the Gateway reference trajectory included the point-mass gravitational influence of the Jupiter barycenter but did not consider SRP [13]. Therefore, the force model for this study incorporated the gravitational forces of the Moon, Earth, Sun, and Jupiter and the force due to SRP. Central body switching was used depending on the proximity to the Moon or Earth. Within the lunar Sphere of Influence (SOI), or less than about 66,150 km in radius from the center of the Moon [25], the Moon was considered the central body, with a gravity field represented with an 8×8 subset of the GRAIL GRGM 1200A lunar gravity model [26]. The other celestial bodies were represented as point masses when the Moon was the central body. Elsewhere in cislunar space, Earth was considered the central body and a 4×4 subset of the JGM-2 gravity model was used to represent its non-spherical gravity field [27]. The other celestial bodies, including the Moon, were represented as point masses when the Earth was the central body.

All debris objects were propagated for one year following the breakup event, unless a stopping condition was encountered. Propagation was terminated early if the altitude above the Moon reached 0 km, neglecting lunar terrain, or if the altitude above the Earth reached 120 km, the approximate start of the Earth's atmosphere. Propagation was also terminated beyond a sphere of a radius of 913,000 km from the center of the Earth [25], which was considered to have represented escape from the Earth-Moon system.

Positions and velocities of all objects were reported once every 300 seconds in four different coordinate frames. The first was the Moon Inertial frame, the "Body Inertial" frame for the Moon available in GMAT [28]. Trajectories in the Moon Inertial frame were used for determining the closest approaches between debris and the Gateway. Trajectories were also reported in two variations of the Earth-Moon rotating frame: one centered at the Moon, and another centered at the Earth-Moon barycenter. The Earth-Moon rotating frame centered at the Moon was used for visualizing lunar-centric trajectories, while the Earth-Moon barycentric rotating frame was used for visualizing motion in the broader cislunar region. Finally, trajectories in the Earth-centered International Cartesian Reference Frame (ICRF) enabled the calculation of Earth-centered orbital elements.

2.5 Debris Simulation Setup

The motion of debris following a breakup event in cislunar space depends on many uncertain variables, including the date and time of the breakup event, the location of the breakup event, the pre-breakup orbit, and the properties of the breakup event. Furthermore, cislunar dynamics are highly complex and nonlinear, especially in a realistic, ephemeris-based trajectory model. This complexity means that trajectories can change dramatically with small changes in initial conditions, making analytical predictions difficult. Monte Carlo simulations are well-suited to handle complex problems of this nature [29]. Therefore, this study used Monte Carlo debris simulations to model random breakup events

Table 1: Cislunar Debris Simulation Setup

Parameter	Value
Deployment Date and Time	Random between 1 Jan 2025 00:00:00 and 1 Jan 2030 00:00:00
Velocity Perturbation	Random magnitude between 0.5-15 m/s and random direction
Time Between Deployment and Breakup	Random between 0-14 days
Breakup Properties	Randomly generated by NASA Standard Breakup Model
Debris Propagation Length	Fixed at 365 days
Number of Simulation Runs	5,000

near the Gateway's NRHO. The results across thousands of breakup events were aggregated to gain insight into the overall risk to the Gateway.

This study aims to simulate cislunar breakup events in the vicinity of the Gateway's NRHO. This type of event could be triggered by the breakup of a spacecraft shortly after deployment from the Gateway. The Gateway will serve as a staging point for future lunar exploration through the Artemis Program when it becomes operational in the late 2020s, with many spacecraft arriving and departing. These spacecraft could include small satellites released from the station and resupply modules [22]. Therefore, the mechanism of the breakup event in this study was an explosion of a spacecraft following deployment from the Gateway. The pre-breakup orbits were all in the vicinity of the Gateway's NRHO, meaning that the results of this study should be generally applicable to any breakup event in an orbit near the Gateway's NRHO, not just those following a deployment.

To model a breakup event in a deployment scenario, the following Monte Carlo simulation design was used:

1. Select a random date and time along the Gateway reference trajectory as the starting point for the simulation. This date and time was between 1 Jan 2025 00:00:00 UTC and 1 Jan 2030 00:00:00 UTC.

2. Perform a random velocity perturbation (or ΔV) in a random direction, representing deployment from the Gateway. The magnitude of the velocity perturbation was between 0.5 and 15 m/s, matching the bounds used in the NRHO deployment study by Davis et al. [22]. The random direction was assigned by selecting a random point on a sphere using the same method as in Equations (8)-(10).

3. Select a random duration between 0 and 14 days. The deployed object was assumed to either have departed the vicinity of the NRHO for its next destination by 14 days or be far enough from the NRHO to no longer pose any risk. A test simulation consisting of 500 breakup events with durations as long as two months supported that breakup events beyond 14 days would pose little collision risk to the Gateway. For breakup events beyond 14 days, no fragments passed within 50 km of the Gateway. Therefore, the 14 day upper limit on the duration was chosen to focus on breakup events that would be most likely to threaten the Gateway.

4. Propagate the deployed object forward by the random duration. For the SRP calculation, the deployed object was assumed to have a mass of 800 kg, a cross-sectional area of 1 m^2, and a coefficient of reflectivity of $c_R = 1.8$. However, these properties have little impact on the propagation due to the small influence of the force due to SRP over a short time period.

5. Simulate a breakup event using the NASA Standard Breakup Model.

6. Propagate the trajectories of all debris particles for one year and determine the closest approach with the Gateway reference trajectory.

7. Repeat this procedure 5,000 times to complete 5,000 runs, i.e., simulate 5,000 breakup events. Plot histograms of the closest approaches to evaluate the risk to the Gateway.

Table 1 summarizes the proposed simulation setup. Fig. 3 marks the breakup locations resulting from this simulation design with red dots. The trajectories of the objects just prior to the breakup event are also shown as lines extending from the breakup location. Breakup events were much more likely to occur at apolune because they were considered uniformly likely in time, and objects in the NRHO spend much more time near apolune.

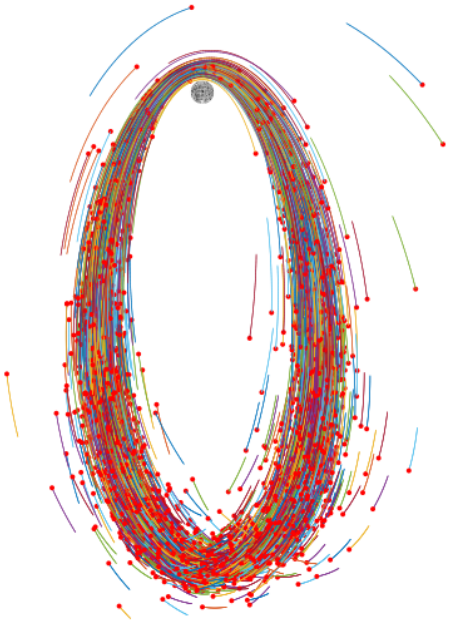

Fig. 3: NRHO Debris Simulation Breakup Locations

Simulating 5,000 breakup events according to this simulation design required the propagation of a total of 1,222,522 debris fragments for one year. This involved substantial computational effort, necessitating the use of High Performance Computing (HPC) resources. Debris fragments were propagated in parallel on HPC resources using Dask, a Python library for parallel computing [30]. This allowed the simulation to complete quickly despite the large number of particles.

2.6 Collision Risk

The observed absolute closest approaches to the Gateway during each of the 5,000 randomly simulated breakup events were aggregated and used to quantify the risk to the Gateway. The frequency of very close approaches to the Gateway can provide insight into the level of collision risk. Existing NASA guidelines for the International Space Station (ISS) classify close approaches within a box 4 km deep, 50 km wide, and 50 km long centered on the spacecraft as potentially requiring a debris avoidance maneuver [31]. However, cislunar space object tracking is currently very limited, and approaches within much larger distances could also generate concern.

This study uses a Monte Carlo approach to evaluate the risk to the Gateway. Monte Carlo simulations require a sufficient number of runs to provide statistically significant results. Therefore, a bootstrap technique similar to that used by Lidtke et al. [32] was used to estimate the uncertainty in the likelihood of close approaches within specified distances of the Gateway. The absolute closest approaches from each of the 5,000 runs were randomly resampled with replacement to generate a new sample of 5,000 runs. The frequency of closest approaches are different in this new sample. This resampling process was repeated 2,000 times to generate 2,000 new samples, and these 2,000 samples can be used to analyze the variation in the observed close approaches and generate 95% confidence intervals. If the number of Monte Carlo runs is sufficient, then there will be little difference between each of the closest approach samples, indicating low uncertainty in the results.

3. RESULTS

The main results of this study include the trajectories of the debris fragments, the collision risk to the Gateway, and the final orbits of the fragments after one year. The following three subsections discuss each of these respective results.

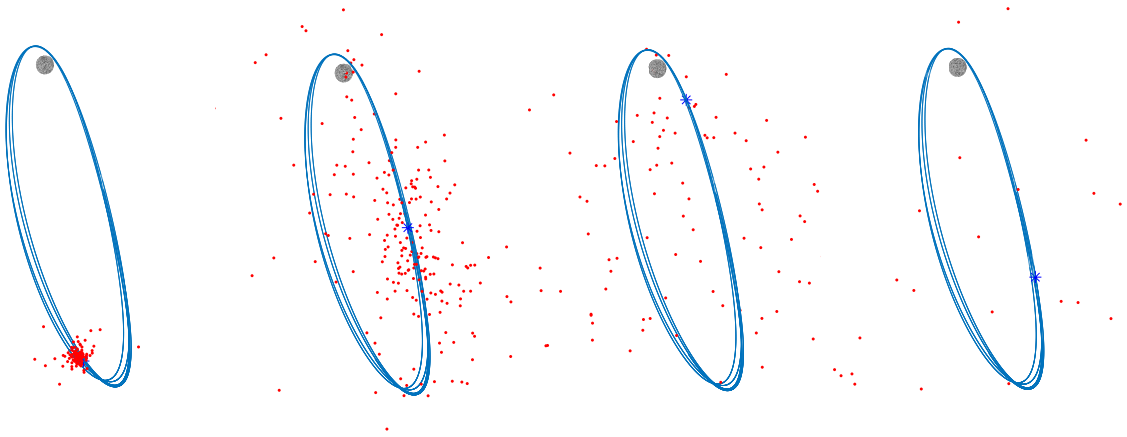

(a) After Five Hours (b) After Three Days (c) After 17 Days (d) After One Month

Fig. 4: Debris Propagation for Single Run, With Gateway Denoted by Blue Asterisk

3.1 Debris Propagation

Fig. 4 plots the positions of debris fragments at specified amounts of time following the breakup event for a single run of the simulation (i.e., a single breakup event). In the example run shown in Fig. 4, the breakup event occurred near the Gateway, and the Gateway is marked with a blue asterisk. While the debris initially followed the Gateway along the NRHO, the fragments spread out within a few days, and fewer fragments remained in the NRHO with each consecutive orbit. After about two weeks, very few fragments were still traveling along the original NRHO, although many were still in the vicinity of the NRHO. After a month, most particles had escaped the vicinity of the NRHO to other regions of cislunar space.

This trend of particles escaping from the NRHO within weeks was typical across all debris simulation runs. Fig. 5a depicts the debris objects near the NRHO after one month for a combined sample of 500 runs. The particles escaping from the NRHO formed a tube extending from the NRHO. Although most objects had escaped from the NRHO, the density of objects near the NRHO was still higher than other regions of cislunar space. This was no longer true by one year: the few remaining particles near the Moon were randomly scattered through the region, with no increase in density near the NRHO. Departures from the NRHO within weeks were also observed in a study of NRHO deployment by Davis et al. [22] and in the study of breakup events in NRHOs by Guardabasso et al. [8]. These results also support the existence of "self-cleaning" properties in NRHOs noted by Guardabasso et al. [8].

3.2 Collision Risk Analysis

The fragment trajectories relative to the Gateway can provide insight into the nature of conjunctions with the station. Fig. 6 plots the fragment trajectories in the Gateway Local-Vertical-Local-Horizontal (LVLH) frame during the first month for the same run shown in Fig. 4. In this LVLH frame, the x-axis points along the vector extending from the Moon to the Gateway, the z-axis points along the Gateway's orbit normal direction relative to the Moon, and the y-axis completes the right-handed coordinate system. The Gateway is fixed at the origin of the coordinate system. The LVLH trajectories demonstrate that objects do not linger in the vicinity of the Gateway, and any transits are relatively brief. This suggests a short-lived risk and a low risk of collision.

The absolute closest approaches to the Gateway during each of the 5,000 runs are plotted in a histogram in Fig. 7. The bin width in the histogram is 100 km. The closest approaches are skewed towards lower values, but there is a large variation in the results, with closest approaches beyond 500 km still relatively common. Fig. 8a depicts the fraction of runs that saw closest approaches within specified distances, and Fig. 8b focuses only on the 0-10 km distances. These results represent the observed probability of an approach within the specified distances during the first year after a breakup event. 95% confidence intervals are also shown on the bar charts, which were generated using the bootstrap resampling process described in Section 2.6. The confidence intervals are small relative to the height of the bars, except for the lower distances shown in Fig. 8b due to the small sample sizes at these values.

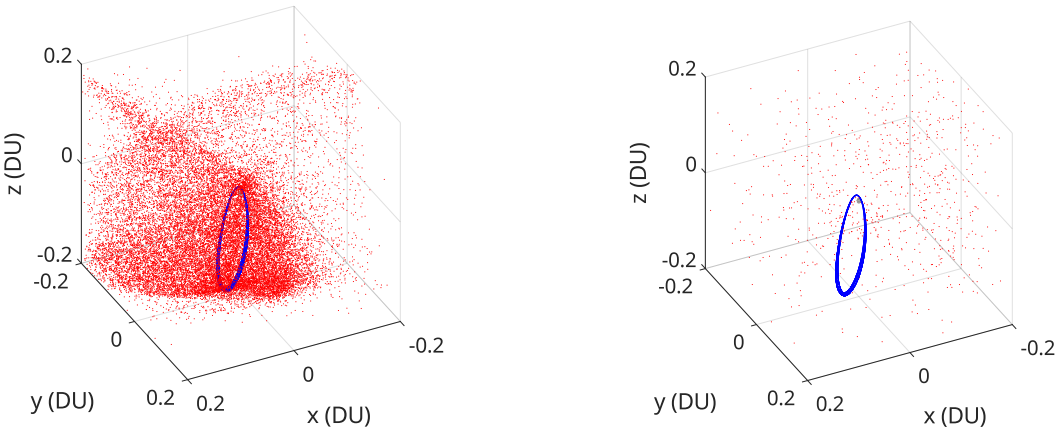

(a) After One Month (b) After One Year

Fig. 5: Debris Near Original NRHO, 500 Run Sample

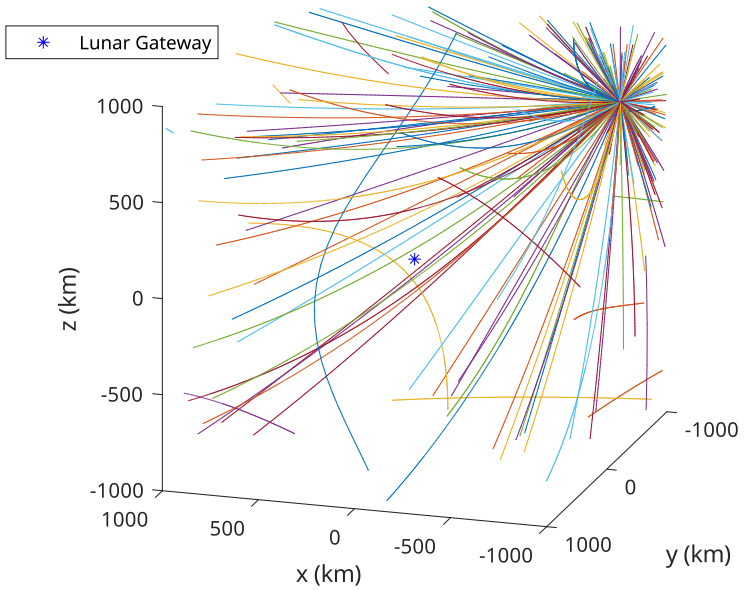

Fig. 6: Debris Trajectories in Gateway LVLH Frame in First Month Month for Single Run

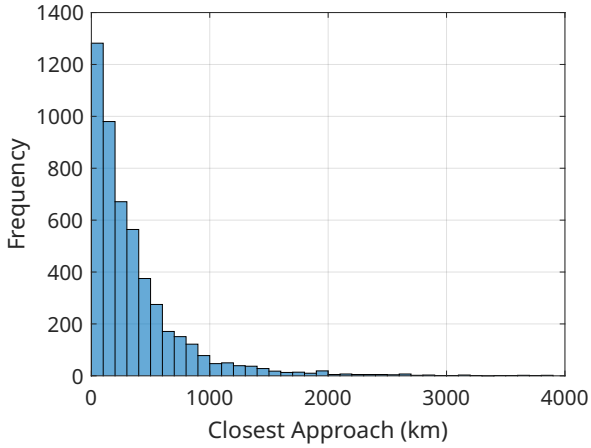

Fig. 7: Histogram of Closest Approaches to Gateway

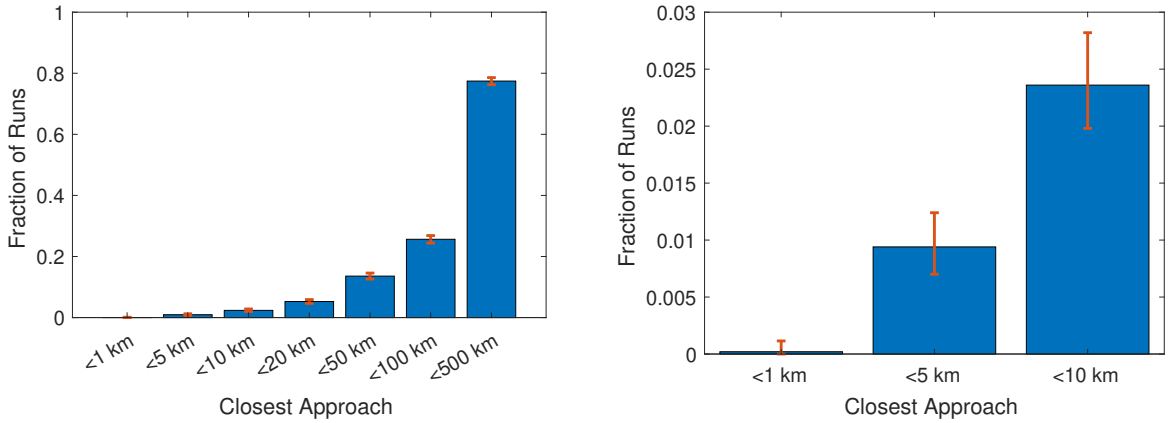

(a) 0-500 km

(b) 0-10 km

Fig. 8: Fraction of Closest Approaches Within Specified Distances

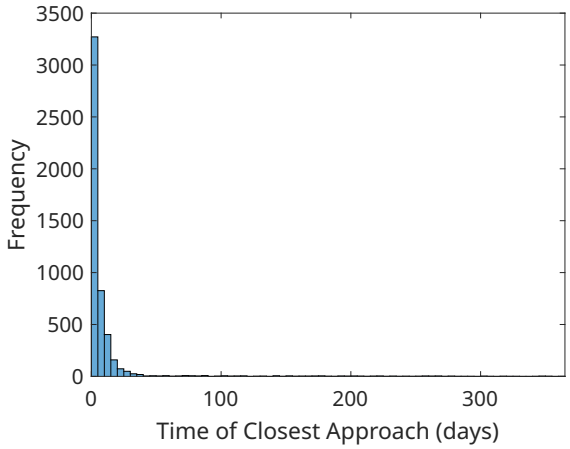

Fig. 9: Histogram of Times of Closest Approaches to Gateway

The closest approach to the Gateway across the 5,000 runs was 0.785 km, and this was the only observed approach within 1 km. The lack of conjunctions within 1 km makes it difficult to infer the exact probability of collision with the Gateway, but the chances appear to be low, likely well below 1 in 5,000. Approaches within 5 km occurred in 0.9% of runs, and approaches within 10 km occurred in 2.4% of runs. The median close approach was 231.7 km. 77.4% of the runs resulted in conjunctions within 500 km.

While the collision risk to the Gateway was low, the approaches were often close enough to potentially generate significant concern, especially considering tracking limitations in cislunar space. For example, 13.6% of the runs saw close approaches within 50 km, a threshold that could trigger a debris avoidance maneuver according to guidelines for the ISS [31]. While similar guidelines for the Gateway are not yet available, the Gateway might be much more likely to execute a debris avoidance maneuver in this scenario to compensate for much more limited space object tracking capabilities in cislunar space. Debris avoidance maneuvers in NRHOs were previously studied by Davis et al. [21]. These authors found that small maneuvers with hours or days of advance notice could mitigate the risk, although the fuel cost tends to increase as the lead time decreases.

The absolute closest approaches tended to occur within the first few days after the breakup event, as shown in the Time of Closest Approach (TCA) histogram in Fig. 9. The bin width in the histogram is five days. The closest approach occurred within six hours for 23.0% of the runs, within one day for 46.7% of the runs, within one week for 74.2% of the runs, and within two weeks for 89.2% of the runs. The median TCA was 1.57 days. This is consistent with the results of Guardabasso et al. [8], who found that most objects no longer remained in a "valuable region" surrounding the NRHO a few days after the breakup event. The closest approaches occur shortly after the breakup because objects tend to depart the NRHO quickly. This means that the collision risk diminishes rapidly, but short lead times could make it difficult to develop an efficient debris avoidance maneuver.

The simulation results can also provide insight into deployment methods that reduce the collision risk to the Gateway. The relationships between a variety of deployment variables and the closest approach measurements are plotted in Fig. 10. The time from deployment to the breakup event and the deployment ΔV, shown in Figs. 10a and 10b, respectively, had the strongest influence on the closest approach measurements. The closest approaches generally increased as the deployment duration increased due to the tendency of objects to depart the NRHO over time. Similarly, higher deployment ΔVs caused objects to depart from the original NRHO to a greater degree prior to the explosion, leading to a higher absolute closest approach. The relationship was especially strong for deployment ΔVs from 0-4 m/s. Below 4 m/s, the median closest approach was 80.1 km, and above 4 m/s, the median closest approach was 302.6 km. This suggests that requiring deployment ΔVs to be above 4 m/s could be a strategy to reduce the risk to the Gateway in the event of a breakup.

Fig. 10c depicts the relationship between the miss distances and the deployment ΔV direction measured as an angle relative to the velocity vector. The approaches were slightly closer when the ΔV was applied in a direction perpendicular to the velocity vector, likely because these maneuvers would change the orbit the least, causing the object to remain

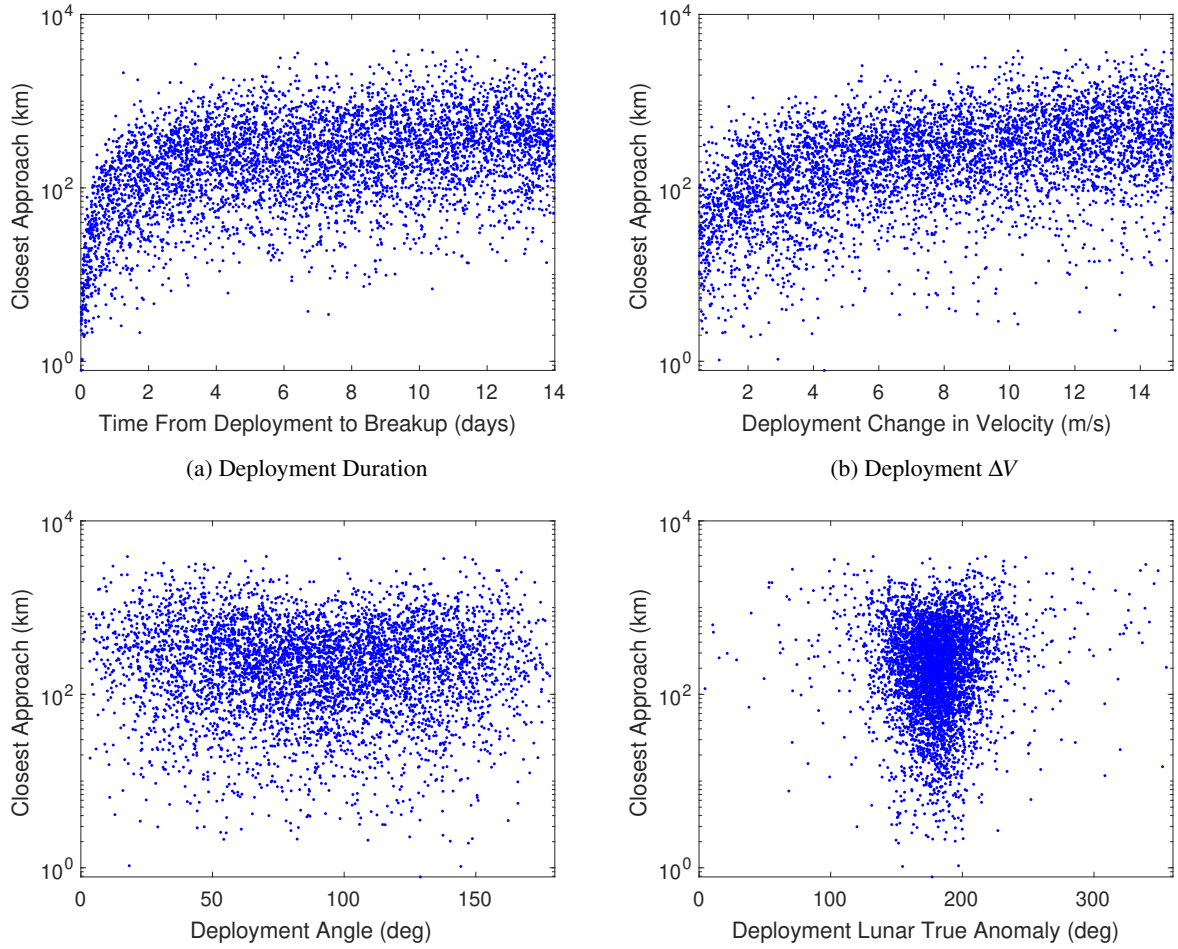

(a) Deployment Duration

(b) Deployment ΔV

(c) Deployment Angle

(d) Deployment True Anomaly

Fig. 10: Correlations Between Deployment Parameters and Closest Approaches

in the NRHO for a longer time. Deployment ΔVs in the same direction as the velocity vector or opposite the velocity vector resulted in slightly more distant conjunctions because these maneuvers cause faster departure from the NRHO. There also appears to be a slight relationship between the lunar true anomaly and the closest approaches, as shown in Fig. 10d, with deployments closer to apolune tending to lead to closer approaches. This would be consistent with Davis et al. [22], who found that the fastest departure from the NRHO occurs for maneuvers in the velocity direction at perilune. However, the sample size is small close to perilune. This is due to the simulation design, which considered deployments to be equally likely in time, and the spacecraft spends much more time at apolune. Future simulations could model different deployment strategies, such as deployment only at perilune, to determine if they reduce the risk to the Gateway.

3.3 Debris Final States

Fig. 11 plots the cumulative fraction of particles that had exited the simulation over time across all 5,000 runs. Particles were considered to have left the simulation if they impacted the Moon, impacted the Earth, or escaped the Earth-Moon system. Many lunar impacts occurred at the beginning of the simulation due to objects placed on lunar impact trajectories by the explosion. The rate at which objects impacted the Moon varied on a cycle approximately matching the period of the Gateway's orbit, or 6.562 days on average [13]. Lunar impacts became far less likely after about 25 days as objects escaped the NRHO. Many fragments began to escape from the Earth-Moon system after about 22 days, and the fraction that had escaped continued to increase through the end of the simulation. Of the original 1,222,522 particles across all runs, 246,018 particles impacted the Moon (20.1%), 80 particles impacted the Earth

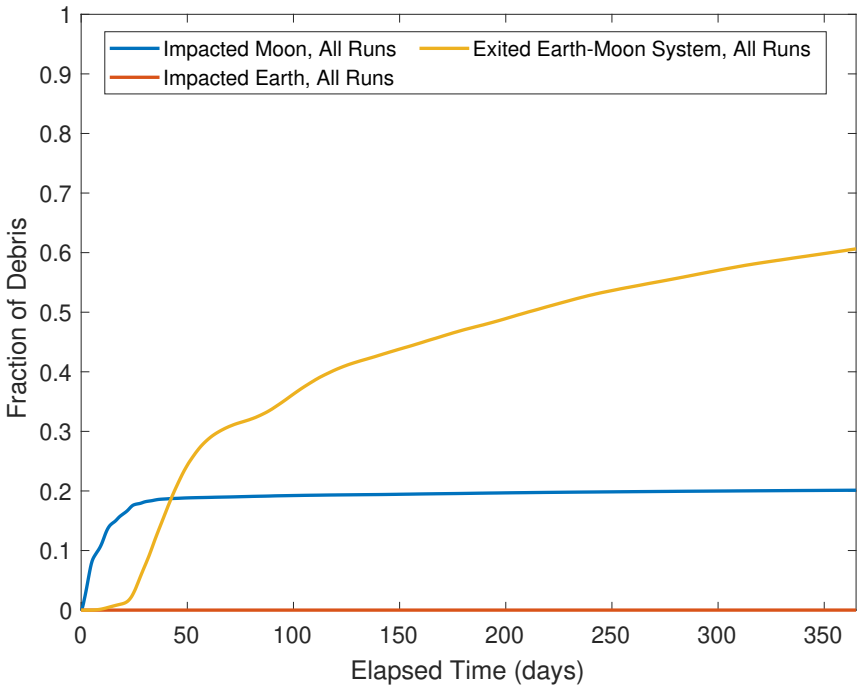

Fig. 11: Fraction of Particles Exiting Simulation Over Time

(0.00654%), and 741,244 particles escaped the Earth-Moon system (60.6%). These results are very similar to those obtained by Guardabasso et al. [8], but lunar impacts in the aggregate results of this study occurred more gradually due to the larger number of fragments propagated and the random nature of the breakup events.

Lunar impacts were more likely in a region in the northern hemisphere of the Moon centered at approximately 42°N, 72°E. Fig. 12 provides a heat map of the locations of lunar surface impacts, with the Gateway reference trajectory's lunar ground track from the years 2025 to 2030 overlaid in black. The impact accumulation is below the Gateway's ground track just prior to perilune. The impacts appear slightly skewed to the left of the ground track, perhaps due to the rotation of the Moon and the time difference between the original ground track and the time at which objects intersect the Moon. Guardabasso et al. [8] appear to have observed an accumulation of lunar impacts at the same location, showing that the impact accumulation is still present even when a larger range of epochs, initial states, and breakup properties are considered. This location does not overlap with potential lunar base sites near the lunar south pole [33], likely indicating low risk to future lunar surface infrastructure from a breakup event near the Gateway's NRHO.

Across all 5,000 runs, a total of 235,210 particles, or 19.2%, remained orbiting in cislunar space. A heat map of the final states of these objects after one year is provided in Fig. 13. The ZVC associated with a Jacobi Constant of 3.05, the approximate Jacobi Constant of the original NRHO, is marked on the plot. There is an excellent correlation between the final states of the particles and the ZVC. An inner ring is clearly visible just inside the ZVC, and a fainter outer ring is present just outside the ZVC. Density was the highest near the opening of the ZVC from the L_1 Lagrange point to the Moon. Fewer particles ended inside the ZVC, but some could still do so due to the addition of energy from the deployment and the breakup event. Very few particles ended near Earth, forming a hole around the Earth in Fig. 13. Few particles had perigees close to the Earth, and those that did likely traversed near-Earth space quickly, spending the majority of the time at apogee.

Some fragments ended the simulation in space near the Earth or Moon. At one year, about 0.6% of all fragments were in space near the Moon within twice the Gateway's apolune (about 142,000 km), while about 4.7% of the fragments were within 7X GEO (about 295,148 km). The Gabbard diagrams in Figs. 14a and 14b plot the apsides and periods of the objects that ended near the Moon and Earth, respectively. The risk to spacecraft near the Earth or Moon from these

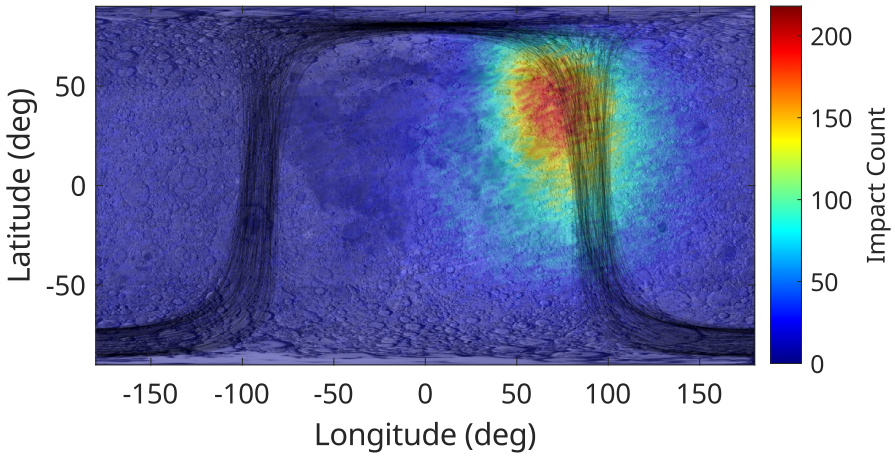

Fig. 12: Heat Map of Lunar Surface Impact Locations, With Gateway Ground Track Overlaid in Black

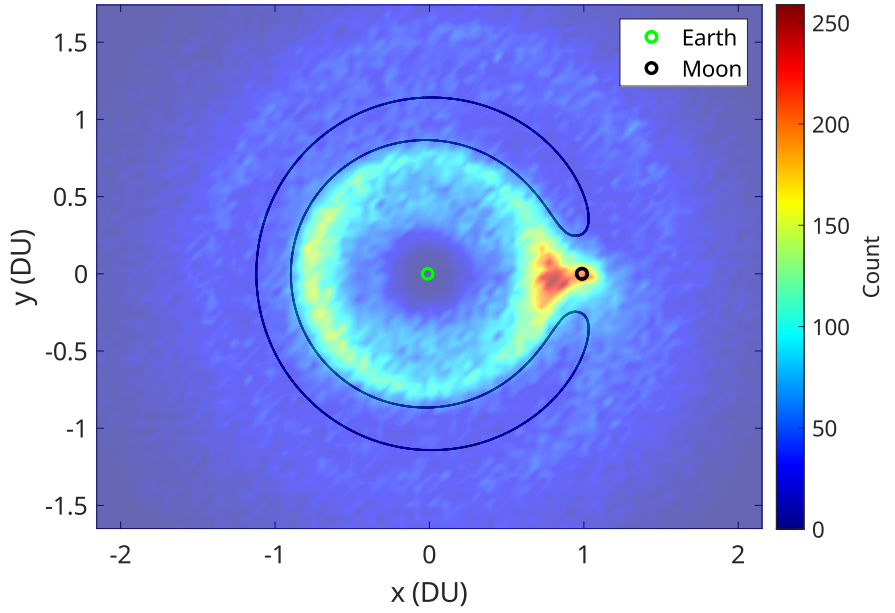

Fig. 13: Heat Map of Final States After One Year in Earth-Moon Barycentric Rotating Frame, With ZVC for Jacobi Constant of 3.05

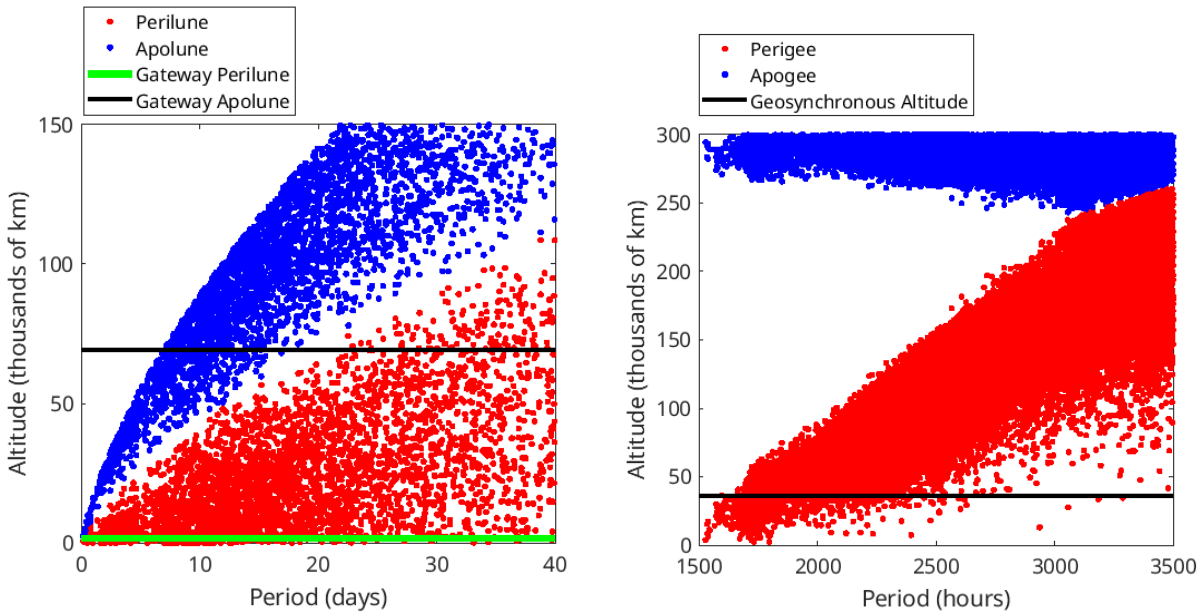

(a) Particles Near Moon (<2X Gateway Apolune)

(b) Particles Near Earth (<7X GEO)

Fig. 14: Gabbard Diagrams After One Year

fragments would be very low. While many objects achieved Earth-centric orbits, only about 0.06% of all fragments had a perigee within GEO. The lack of close approaches to the Earth also led to very few Earth impacts. Of the fragments with a perigee within GEO, the inclinations relative to the Earth's equator were between approximately 0 and 70 degrees. The average inclination was 29 degrees, which is close to the Gateway reference trajectory's average inclination relative to the Earth.

4. CONCLUSION

This study presented the results of Monte Carlo simulations of spacecraft breakup events near the Lunar Gateway's NRHO, focusing on modeling a scenario in which an object suffers a breakup event shortly after deployment from the station. In total, 5,000 breakup events consisting of 1,222,522 fragments with randomly generated initial conditions were simulated and the debris propagated for one year. This provided a robust sample with which to calculate statistics on the likelihood of collision between debris and the Gateway. Furthermore, the simulation results also provided insight into the number of impacts with the Earth and Moon and the distribution of objects in cislunar space after one year.

The simulations observed a low overall risk of collision with the Gateway, with conjunctions within 10 km observed in only 2.4% of the runs and a median absolute closest approach of 232 km. However, a maneuver to avoid debris would very likely be required, especially considering tracking limitations in cislunar space. Close approaches within 50 km, a level that would trigger discussions of a possible debris avoidance maneuver according to ISS guidelines [31], occurred in 13.6% of the runs. Close approaches were typically observed quickly, with a median TCA of 1.57 days, potentially making a debris avoidance maneuver time-sensitive. The collision risk dropped dramatically within days to a couple weeks as fragments quickly departed the NRHO. Based on these results, there would be minimal long-term risk to the Gateway and no risk of debris accumulation in the NRHO.

Nearly all objects had escaped from the NRHO after one year and ended the simulation elsewhere in cislunar space. After one year, about 20% of the fragments impacted the Moon and about 61% escaped the Earth-Moon system. Lunar impacts were heavily skewed towards the northern hemisphere of the Moon, below the Gateway's ground track just prior to perilune. Very few Earth impacts were observed. The fragments remaining in cislunar space were mostly distributed around the ZVC associated with the Jacobi Constant of the original NRHO. Only about 0.06% of the fragments ended the simulation with a perigee within GEO, suggesting a low risk to spacecraft near Earth.

Overall, this research provides a quantification of the risk from a breakup event near the Gateway's NRHO, enabling insight into the importance of avoiding such a scenario and operational strategies to reduce the risk. Although the risk of collision with the Gateway is low, this type of event would likely generate significant concern in the absence of robust cislunar object tracking capabilities, and development of strategies to reduce the risk may be required. This study found that deployment ΔVs above 4 m/s would likely be an effective strategy to reduce the likelihood of conjunctions, and deployment at perilune may also reduce the risk. Future studies could investigate the influence of specific deployment methods on the close approaches to the Gateway to identify the safest deployment strategies. Furthermore, the methods used in this study could be applied to simulate breakup events in other useful cislunar orbits, such as Distant Retrograde Orbits (DROs), to evaluate the risk across a variety of environments.

5. REFERENCES

[1] Kaitlyn Johnson. *Fly me to the Moon: worldwide cislunar and lunar missions*. Center for Strategic and International Studies, 2022. Available at `https://www.csis.org/analysis/fly-me-moon-worldwide-cislunar-and-lunar-missions` (10 Nov 2022).

[2] White House Office of Science and Technology. National cislunar science and technology strategy. Available at `https://www.whitehouse.gov/ostp/news-updates/2022/11/17/fact-sheet-first-national-cislunar-science-technology-strategy/` (6 Jan 2023), Nov 2022.

[3] George E. Pollock IV and James A. Vedda. Cislunar stewardship: Planning for sustainability and international cooperation. Available at `https://csps.aerospace.org/papers/cislunar-stewardship-planning-sustainability-and-international-cooperation` (6 Jan 2023), Jun 2020.

[4] Nathan R. Boone. Cislunar debris propagation following a catastrophic spacecraft mishap. Master's thesis, Air Force Institute of Technology, 2021. AFIT-ENY-MS-21-M-289.

[5] Nathan R. Boone and Robert A. Bettinger. Cislunar debris propagation following a catastrophic spacecraft mishap. In *AIAA SciTech 2021 Forum*, 2021. AIAA 2021-0102.

[6] Nathan R. Boone and Robert A. Bettinger. Debris propogation following a spacecraft mishap at the collinear Earth-Moon Lagrange points. In *2021 IEEE Aerospace Conference*, 2021.

[7] Adam P. Wilmer, Nathan R. Boone, and Robert A. Bettinger. Debris propagation and spacecraft survivability assessment for catastrophic mishaps occurring in cislunar periodic orbits. *Journal of Space Safety Engineering*, 9(2):207–222, 2022.

[8] Paolo Guardabasso, Despoina K. Skoulidou, Lorenzo Bucci, Francesca Letizia, Stijn Lemmens, Marie Ansart, Xavier Roser, Stéphanie Lizy-Destrez, and Grégoire Casalis. Analysis of accidental spacecraft break-up events in cislunar space. *Advances in Space Research*, 2023.

[9] J.C. Dolado-Perez, Carmen Pardini, and Luciano Anselmo. Review of uncertainty sources affecting the long-term predictions of space debris evolutionary models. *Acta Astronautica*, 113:51–65, 2015.

[10] Nathan Boone and Robert Bettinger. Simulation of debris events in selected low lunar orbits. *The Journal of the Astronautical Sciences*, 70(3):16, 2023.

[11] Victor Szebehely. *Theory of Orbits: The Restricted Problem of Three Bodies*. Academic Press, 1967.

[12] Jeffrey S Parker and Rodney L Anderson. *Low-energy lunar trajectory design*, volume 12. John Wiley & Sons, 2014.

[13] David E. Lee. White paper: Gateway destination orbit model: A continuous 15 year NRHO reference trajectory. Available at `https://ntrs.nasa.gov/citations/20190030294` (6 Jan 2023), Aug 2019.

[14] N.L. Johnson, P.H. Krisko, J.-C. Liou, and P.D. Anz-Meador. NASA's new breakup model of EVOLVE 4.0. *Advances in Space Research*, 28(9):1377–1384, 2001.

[15] Nathan R. Boone and Robert A. Bettinger. Debris collision risk analysis following simulated cislunar spacecraft explosions. *Journal of Spacecraft and Rockets*, 60(2):668–684, 2023.

[16] Stefan Frey and Camilla Colombo. Transformation of satellite breakup distribution for probabilistic orbital collision hazard analysis. *Journal of Guidance, Control, and Dynamics*, 44(1):88–105, 2021.

[17] Paula H. Krisko. Proper implementation of the 1998 NASA breakup model. *Orbital Debris Quarterly News*, 15(4):4–5, 2011.

[18] Eric W. Weisstein. Sphere point picking. `https://mathworld.wolfram.com/SpherePointPicking.html` (27 Jun 2022).

[19] Luciano Anselmo and Carmen Pardini. Long-term dynamical evolution of high area-to-mass ratio debris released into high Earth orbits. *Acta Astronautica*, 67(1):204–216, 2010.
[20] Steven P. Hughes, Rizwan H. Qureshi, Steven D. Cooley, and Joel J. Parker. Verification and validation of the General Mission Analysis Tool (GMAT). In *AIAA/AAS Astrodynamics Specialist Conference*, 2014.
[21] Diane C. Davis, Emily M. Zimovan-Spreen, Stephen T. Scheuerle, and Kathleen C. Howell. Debris avoidance and phase change maneuvers in Near Rectilinear Halo Orbits. In *AAS/AIAA Space Flight Mechanics Meeting*, 2022. AAS 22-068.
[22] Diane C. Davis, Kenza K. Boudad, Sean M. Phillips, and Kathleen C. Howell. Disposal, deployment, and debris in Near Rectilinear Halo Orbits. In *AAS/AIAA Space Flight Mechanics Meeting*, 2019. AAS 19-466.
[23] Kenza K. Boudad, Diane C. Davis, and Kathleen C. Howell. Disposal trajectories from Near Rectilinear Halo Orbits. In *AAS/AIAA Space Flight Mechanics Meeting*, 2018. AAS 18-289.
[24] Diane C. Davis, Rolfe J. Power, Kathleen C. Howell, and Jeffrey P. Gutkowski. Lunar impact probability for spacecraft in Near Rectilinear Halo Orbits. In *AAS/AIAA Space Flight Mechanics Meeting*, 2018. AAS 21-452.
[25] G. A. Chebotarev. Gravitational spheres of the major planets, moon and sun. *Soviet Astronomy*, 7(5):618–622, Apr 1964.
[26] National Aeronautics and Space Administration. Lunar gravity field: GRGM1200A. Available at `https://pgda.gsfc.nasa.gov/products/50` (11 Dec 2022).
[27] R. S. Nerem, F. J. Lerch, J. A. Marshall, E. C. Pavlis, B. H. Putney, B. D. Tapley, R. J. Eanes, J. C. Ries, B. E. Schutz, C. K. Shum, M. M. Watkins, S. M. Klosko, J. C. Chan, S. B. Luthcke, G. B. Patel, N. K. Pavlis, R. G. Williamson, R. H. Rapp, R. Biancale, and F. Nouel. Gravity model development for TOPEX/POSEIDON: Joint Gravity Models 1 and 2. *Journal of Geophysical Research: Oceans*, 99(C12):24421–24447, 1994.
[28] Steve Hughes. General Mission Analysis Tool (GMAT) technical specifications. NASA Technical Reports Server (1 Jan 2007).
[29] J.G. Amar. The Monte Carlo method in science and engineering. *Computing in Science & Engineering*, 8(2):9–19, 2006.
[30] Matthew Rocklin. Dask: Parallel computation with blocked algorithms and task scheduling. In *Proceedings of the 14th Python in Science Conference*, 2015.
[31] Eugene Stansbery. NASA orbital debris program. Available at `https://ntrs.nasa.gov/api/citations/20130010239/downloads/20130010239.pdf` (23 Jul 2023), Mar 2013.
[32] Aleksander A. Lidtke, Hugh G. Lewis, and Roberto Armellin. Statistical analysis of the inherent variability in the results of evolutionary debris models. *Advances in Space Research*, 59(7):1698–1714, 2017.
[33] Brian Baker-McEvilly, Sebastian Doroba, Annika Gilliam, Franco Criscola, David Canales, Carolin Frueh, and Troy Henderson. A review on hot-spot areas within the cislunar region and upon the Moon surface, and methods to gather passive information from these regions. In *AAS/AIAA Space Flight Mechanics Meeting*, 2023. AAS 23-194.